Iranian Journal of Astronomy and Astrophysics
Vol. 2, No. 2
©Available online at http://journals.du.ac.ir

Iranian Journal of Astronomy and Astrophysics

Effects of shear and bulk viscosity on head-on collision of localized waves in high density compact stars

Azam Rafiei · Kurosh Javidan · Mohammad Ebrahim Zomorrodian
Department of Physics, Ferdowsi University of Mashhad, 91775-1436, Mashhad, Iran

Abstract. Head on collision of localized waves in cold and dense hadronic matter with and without shear and bulk viscosities is investigated. Non-relativistic dynamics of propagating waves is studied using the hydrodynamics description of the system and suitable equation of state. It will be shown that the localized waves are described by solutions of the Burgers equation. Simulations show that the propagating waves in viscous media travel longer distances in comparison with inviscid similar fluids. In this way, the traveling distance of localized waves is a suitable criterion for evaluating the viscosity of hadronic fluids.

I. Introduction

It is believed that nuclear matters are created in the core of compact stars and in heavy ion collisions [1, 2]. There are some similarities between these two situations, like high density and also some contrasts such as difference in the medium temperature. Since the temperature in the core of compact stars is approximately a few mega electron volts, cold nuclear matter exists in such these places; on the contrary high temperature (a few tens of mega electron volts) nuclear matter can be produced after the relativistic heavy ion collisions. Phase transition from confined hadronic matter to deconfined quark gluon plasma (QGP) has been observed in both situations [1]. In the case of compact star, formation of the QGP regularly is started at the center of a compact star by increasing of its density above the critical density. Afterward the new phase will spread to the environs.
Because of inaccessibility of the interior of compact stars as a unique natural sample at very dense ($5-10$ times larger than normal saturation density, $\rho_0 = 0.16fm^{-3}$) and very low temperature in terrestrial laboratory [2, 3], analysis of dynamic behavior of hadronic matter is investigated by heavy ion collisions [1, 4, 5]. Neutron stars and white dwarfs are two kinds of compact stars [6].Studying the propagation and collision of localized waves in such these media, produces valuable information about the stars formation and the dynamics of compact objects [7]. Propagation and interaction of small amplitude localized waves in the form of shock profilesare investigated in this paper.
A neutron star is characterized by the following conditions: the mass is nearly $1.5M_{\odot}$ ($M_{\odot}$ is the mass of sun), the radius is approximately $10Km$ and its initial temperature is about $10^{11}K$ [8]. At the center of the star the energy density upon c^2 changes from 10^{14} up to $10^{15}g.cm^{-3}$ and it reaches to zero at the surface of the star. For a typical neutron star, five different regions can be distinguished. I) Outer crust by $10^4 \leq \rho \leq 10^{11}g.cm^{-3}$, where contains lattice of neutron-rich nuclei in a free gas of (relativistic) electrons. II) The neutron drip line with the density $\rho \approx 10^{11}g.cm^{-3}$. Because of weakly bounding in this region, the neutrons are able to drip out of the nuclei and they become free increasingly. III) Inner crust (free neutron phase) with $10^{11} \leq \rho \leq 10^{14}g.cm^{-3}$, where neutron-rich nuclei are

situated in a free gas of electrons and neutrons. *IV*) The outer core with $\rho \approx 5 \times 10^{14} g.cm^{-3}$ which contains neutrons, electrons, protons and muons in the form of a homogeneous liquid. *V*) Finally unfamiliar inner core with ρ several times $10^{14} g.cm^{-3}$. It is expected that the Fermi energies of the constituent particles could exceed the rest masses of heavier particles and therefore hyperons can be produced in this region [3]. Transition to deconfined quark matter most likely occurs in this situation [8].

Equation of state (EoS) plays an important role to investigate the behavior of matter in different phases. The EoS in hadronic phase is obtained from the famous nonlinear Walecka model. In the QGP phase the Bag model is utilized [9, 10, 11].

There are two different approaches to describe the hadronic matter. In the "microscopic approach" particle trajectories are pursued, while in the "macroscopic view" the hydrodynamic variables like temperature, pressure and velocity of the fluid are specified during the evolution of the system [12]. Generally there is not any precise knowledge on the microscopic details of reactions [13], especially where the nucleon mean free path is shorter than the dimension of the system [12]. In this situation the system behaves like a perfect fluid with a low viscosity (in QGP phase) or a viscous fluid (for hadron gas) [14, 15]. Hence the relativistic hydrodynamics model is constructed based on the local equilibrium [13, 16], however non-equilibrium degrees of freedom can be added to the problem in different ways. In this framework the variables of the model are the energy-momentum tensor, $T_{\mu\nu}$, net particle density, ρ, and the entropy density, S_μ. The relativistic fluid equation of state is obtained using the local conservation of energy-momentum, the relativistic continuity equation and considering the first law of thermodynamics [12, 15, 16, 17, 18, 19, 20] .

The investigation of localized anisotropies and perturbations help us for finding valuable information about the nature of the hydrodynamics medium, where the waves are propagated. There exist four different sources of density fluctuations which create localized waves propagating in the medium. These are: 1)initial state fluctuations, 2)hydrodynamic fluctuations, 3)fluctuations induced by hard processes and 4)freeze-out fluctuations. Quantum fluctuations in the densities of two colliding nuclei supplemented with energy fluctuations are called initial state fluctuations. Local thermal fluctuations of the energy density and flow velocity produce hydrodynamic fluctuations. Energy loss due to propagation of energetic partons causes hard process fluctuations. Finally there are event-by-event fluctuations during and after the freeze-out stage which are called freeze-out fluctuations [15, 21, 22, 23]. Such these perturbations are able to create nonlinear localized waves in the medium which can be detected and also studied during the evolution of the system. Therefore, the propagation of nonlinear waves and their collisions are very interesting subjects.

Nonlinear solitary waves utilize in various branches of physics [24, 25]. They are unique solutions which travel a long distance in nonlinear medium while save their shapes. Behavior of solitary waves during their collisions provides interesting information about the medium such as phase shift and traveling distance of the waves after the collision. Indeed, after the collision of two solitons, they emerge out with almost the same shapes and velocities that they entered in, but with different relative phase shifts. The phase shifts are functions of the soliton characters and also the medium properties [26, 27, 28]. Propagation of localized waves in super dense hadronic matters has been investigated in non-relativistic and viscose medium. But interaction of localized waves and especially head-on collision of solitary waves have not been studied before. Motivated by these situations, propagation of localized waves due to fluctuations and their head on collisions in hadronic gas are investigated in this paper.

In the next section the equations which govern the dynamics of hadron gas are obtained from the Lagranginan density of the medium particles. Thermodynamic relations for these medium will be introduced in this section too. The standard perturbation method in head-on collision will be presented in the third section. The Burgers equations are derived for

propagation of localized perturbations in hadron gas and the phase shifts of traveling waves, after the collision will be obtained in this section. The effects of viscosity on the behavior of localized waves are studied using numerical stimulations in the forth section. Finally, conclusions and some remarks are presented in the last section.

II. Hadronic matter

Dynamics of particles in a hadronic matter can be described using the nonlinear mean field theory (NMFL) approximation [29]. According to the chiral power counting, the famous Walecka model characterizes the properties of cold and high density nuclear matter which exist in the super dense nuclear matter, neutron stars and supernovas. This model is also recognized as (σ, ω) model or quantum hydrodynamics model. Based on the principal specifications of head-on collisions, interaction between two nucleons happens via the exchange of virtual σ and ω mesons. These mesons prepare the intermediate range attraction and short range repulsion respectively. So the Walecka model [29, 30, 31] is defined by the following Lagrangian density (1)

$$\begin{aligned}\mathcal{L} &= \overline{\psi}\left[\gamma_\mu\ (i\partial^\mu - g_\omega\omega^\mu) - (M - g_\sigma\sigma)\right]\psi + \frac{1}{2}\left(\partial_\mu\sigma\partial^\mu\sigma - m_\sigma^2\sigma^2\right) \\ &\quad -\frac{1}{4}F_{\mu\nu}F^{\mu\nu} + \frac{1}{2}m_\omega^2\omega_\mu\omega^\mu - \frac{\kappa}{3}\sigma^3 - \frac{\lambda}{4}\sigma^4 \end{aligned} \tag{1}$$

where nucleons (baryon fields), ψ, neutral Lorentz scalar field, σ, and neutral vector meson field, ω_μ, with their couplings and masses are the degrees of freedom for the theory. The expression $M^* = M - g_\sigma\sigma$ is the nucleon effective mass and the weights of the nonlinear scalar terms are shown by the couplings κ and λ while $F_{\mu\nu} = \partial_\mu\omega_\nu - \partial_\nu\omega_\mu$. According to the NMFT the equation of state are driven considering the meson fields act classically [15, 32] as follow

$$\omega_\mu \to <\omega_\mu> \equiv \delta_{\mu 0}\ \omega_0 \quad ,\ \sigma \to <\sigma> \equiv \sigma_0 \tag{2}$$

In which σ_0 and ω_0 are constant. Assuming there is spatially unlimited nuclear matter in statistical, homogeneous and isotropic state at zero temperature where the intense baryonic sources couple to meson fields strongly. In this case the above mentioned classical assumption is an acceptable approach. Thus the equation of motion are driven from [15, 32]

$$m_\omega^2\omega_0 = g_\omega\psi^\dagger\psi \tag{3}$$

$$m_\sigma^2\sigma_0 = g_\sigma\overline{\psi}\psi - \kappa\sigma_0^2 - \lambda\sigma_0^3 \tag{4}$$

$$\left[i\ \gamma_\mu\partial^\mu - g_\omega\gamma_0\omega_0 - (M - g_\sigma\sigma_0)\right]\psi = 0 \tag{5}$$

The baryon density, ρ_B, is introduced by $\psi^\dagger\psi \equiv \rho_B = \frac{\gamma}{6\pi^2}k_F^3$ where k_F is the Fermi momentum. Therefore, the vector Meson ω_0 will be derived by using equation (3) in terms of baryon density as $\omega_0 = g_\omega\rho_B/m_\omega$. The Dirac Eq. which is performed through the equation (5) couples the nucleons to the vector mesons. From the calculations implemented in [15] the corresponding energy density could be derived using the average of the energy-momentum tensor [15, 32] as follows

$$\begin{aligned}\varepsilon &= \frac{g_\omega^2}{2m_\omega^2}\rho_B^2 + \frac{m_\sigma^2}{g_\sigma^2}(M - M^*) + \kappa\frac{(M - M^*)^3}{3g_\sigma^3} \\ &\quad +\lambda\frac{(M - M^*)^4}{4g_\sigma^4} + \frac{\gamma}{(2\pi)^3}\int_0^{k_F} d^3k\sqrt{\overrightarrow{k}^2 + M^{*2}}\end{aligned} \tag{6}$$

where the nucleon degeneracy factor is shown by γ that equals to 4 . In the above equation, the integral term takes into account the fermion contribution. The self-consistency relation obtained from the minimization of $\varepsilon(M^*)$ with respect to M^* determines the nucleon effective mass as follow

$$\begin{aligned} M^* &= M - \frac{g_\sigma^2}{m_\sigma^2}\frac{\gamma}{(2\pi)^3}\int_0^{k_F} d^3k\sqrt{\overrightarrow{k}^2 + M^{*2}} \\ &\quad + \frac{g_\sigma^2}{m_\sigma^2}\left[\frac{\kappa}{g_\sigma^3}(M-M^*)^2 + \frac{\lambda}{g_\sigma^4}(M-M^*)^3\right] \end{aligned} \tag{7}$$

The following numerical values for masses and couplings are used for calculation from [15, 32] $M = 939\ MeV,\ m_\omega = 783\ MeV,\ m_\sigma = 550\ MeV,\ \kappa = 13.47 fm^{-1},\ g_\omega = 9.197,\ g_\sigma = 8.81,\ and \lambda = 43.127$. The baryon density ρ_B varies in the range of $\rho_0 \leq \rho_B \leq 2\rho_0$ in which $\rho_0 = 0.17 fm^{-3}$ is the nuclear baryon density. If the equation (7) is numerically solved, the nucleon effective mass in term of baryon density will be obtained. In this way, the energy density as a function of baryon density is achieved in [15, 32]

$$\begin{aligned} \varepsilon &= \left(0.1\frac{m_\sigma^2}{g_\sigma^2} + 0.04\frac{\kappa}{g_\sigma^3} + 0.01\frac{\lambda}{g_\sigma^4}\right) + \left(4 + 2\frac{m_\sigma^2}{g_\sigma^2} + \frac{\kappa}{g_\sigma^3} + 0.43\frac{\lambda}{g_\sigma^4}\right)\rho_B \\ &\quad + \left(-3.75 + \frac{g_\omega^2}{2m_\omega^2} + 8\frac{m_\sigma^2}{g_\sigma^2} + 7.6\frac{\kappa}{g_\sigma^3} + 5.42\frac{\lambda}{g_\sigma^4}\right)\rho_B^2 \\ &\quad + \left(21.26\frac{\kappa}{g_\sigma^3} + 30.35\frac{\lambda}{g_\sigma^4}\right)\rho_B^3 + \left(63.73\frac{\lambda}{g_\sigma^4}\right)\rho_B^4 \\ &\quad -1.22\rho_B^{\frac{8}{3}} + 2.61\ \rho_B^{\frac{5}{3}} - 1.4\rho_B^{2/3} \end{aligned} \tag{8}$$

Infinitely high density hadronic plasmas with shear viscosity, υ, and bulk viscosity, ζ, are characterized by the continuity and non-relativistic Navier-Stokes equations

$$\frac{\partial\rho}{\partial t} + \nabla.(\rho\overrightarrow{v}) = 0 \tag{9}$$

and

$$\frac{\partial v^i}{\partial t} + v^k\frac{\partial v^i}{\partial x^k} = -\frac{1}{\rho}\frac{\partial p}{\partial x^k} - \frac{1}{\rho}\frac{\partial \Pi^{ki}}{\partial x^k} \tag{10}$$

with

$$\Pi^{ki} = -\upsilon\left(\frac{\partial v^i}{\partial x^k} + \frac{\partial v^k}{\partial x^i} - \frac{2}{3}\delta^{ki}\frac{\partial v^l}{\partial x^l}\right) - \zeta\delta^{ki}\frac{\partial v^l}{\partial x^l} \tag{11}$$

where Π^{ki} is the viscous tensor ; $\overrightarrow{v}(t,\overrightarrow{x})$, $p(t,\overrightarrow{x})$ and $\rho(t,\overrightarrow{x})$ are the velocity, pressure and the fluid mass density respectively. Considering $i = l = k = x$ for one dimensional Cartesian case, we have

$$\frac{\partial v_x}{\partial t} + v_x\frac{\partial v_x}{\partial x} = -\frac{1}{\rho}\frac{\partial p}{\partial x} + \frac{1}{\rho}\left(\zeta + \frac{4}{3}\upsilon\right)\frac{\partial^2 v_x}{\partial x^2} \tag{12}$$

$$\frac{\partial\rho_B}{\partial t} + v_x\frac{\partial\rho_B}{\partial x} + \rho_B\frac{\partial v_x}{\partial x} = 0 \tag{13}$$

The mass density and the baryon density are related to each other through $\rho = M\rho_B$, where M is the nucleon mass. The first law of thermodynamic at zero temperature results in

$$d\varepsilon = \mu_B d\rho_B \tag{14}$$

So the chemical potential μ_B is

$$\mu_B = \frac{d\varepsilon}{d\rho_B} \tag{15}$$

Substitution of (14) and (15) into the Gibbs equation at zero temperature leading

$$d\varepsilon + dp = \rho_B d\mu_B + \mu_B d\rho_B \tag{16}$$

This yields to

$$dp = \rho_B d\mu_B \tag{17}$$

and finally we have

$$dp = \rho_B d\left(\frac{\partial \varepsilon}{\partial \rho_B}\right) \tag{18}$$

$$\frac{\partial p}{\partial x} = \rho_B \frac{\partial}{\partial x}\left(\frac{\partial \varepsilon}{\partial \rho_B}\right) \tag{19}$$

Replacing Equations (18) and (19) into (12) results in

$$\rho_B \frac{\partial v_x}{\partial t} + v_x \frac{\partial v_x}{\partial x} = -\frac{1}{M}\rho_B \frac{\partial}{\partial x}\left(\frac{\partial \varepsilon}{\partial \rho_B}\right) + \frac{1}{M}\left(\zeta + \frac{4}{3}\upsilon\right)\frac{\partial^2 v_x}{\partial x^2} \tag{20}$$

And using (8) we have

$$\begin{aligned}
\rho_B\left(\frac{\partial v_x}{\partial t} + v_x \frac{\partial v_x}{\partial x}\right) \quad = \quad & -\frac{1}{M}\left(-7.5 + \frac{g_\omega^2}{m_\omega^2} + 16\frac{m_\sigma^2}{g_\sigma^2} + 15.2\frac{\kappa}{g_\sigma^3} + 10.84\frac{\lambda}{g_\sigma^4}\right) \\
& \rho_B \frac{\partial \rho_B}{\partial x} + \left(127.56\frac{\kappa}{g_\sigma^3} + 182.1\frac{\lambda}{g_\sigma^4}\right) \\
& \rho_B^2 \frac{\partial \rho_B}{\partial x} + \left(764.76\frac{\lambda}{g_\sigma^4}\right)\rho_B^3 \frac{\partial \rho_B}{\partial x} \\
& -5.42\rho_B^{\frac{5}{3}}\frac{\partial \rho_B}{\partial x} + 2.9\rho_B^{\frac{2}{3}}\frac{\partial \rho_B}{\partial x} \\
& +0.33\rho_B^{-\frac{1}{3}}\frac{\partial \rho_B}{\partial x} + \frac{1}{M}\left(\zeta + \frac{4}{3}\upsilon\right)\frac{\partial^2 v_x}{\partial x^2}
\end{aligned} \tag{21}$$

This is the Navier-Stokes equation for the hadron phase [15].

III. Head-on collision in hadronic gas

There are two different types of interaction between solitons in one-dimensional collisions. In an overtaking collision, they move in the same direction with different velocities. Solitons receive a phase shift after the interaction, however their shapes remain almost unchanged. This type of collision can be studied using the inverse scattering method. The other one is head-on collision. It occurs when two solitary waves propagate in the opposite directions. In this situation, in addition to the phase shifts, trajectories of colliding solitons are changed after the collision as well.

Phase shift and the trajectories of interacting solitary waves after collision have been studied by many authors using several methods [24, 26, 27].

The extended version of Poincare-Lighthill-Kuo (PLK) approach based on the standard perturbation method is a well-known and powerful technique which can be used in head on collision interactions. This technique generally is called Reductive Perturbation Method

(RPM) [26, 27, 33]. In this method the nonlinearities, dissipative and dispersive effects are preserved in the wave equations. Conventionally a head on collision problem can be studied by introducing the stretched coordinates

$$\begin{cases} \xi = \sigma\left(x - c_1 t\right) + \sigma^2 P_0\left(\eta,\tau\right) + \sigma^3 P_1\left(\eta,\xi,\tau\right) + \dots \\ \eta = \sigma\left(x + c_2 t\right) + \sigma^2 Q_0\left(\xi,\tau\right) + \sigma^3 Q_1\left(\eta,\xi,\tau\right) + \dots \\ \tau = \sigma^3 t \end{cases} \tag{22}$$

where ξ and η denote the trajectories of two localized waves travelling to the right and left directions respectively and σ is a small expansion parameter. The variables c_1 and c_2 are unknown phase velocities which will be calculated. Initially the dimensionless variables for the baryon density, the fluid velocity and the pressure are defined as:

$$\rho = \frac{\rho_B}{\rho_0}\ ,\ v_x = \frac{v_x}{c_s}\ \ ,\ p = \frac{p}{p_0} \tag{23}$$

Where ρ_0, c_s and p_0 respectively are the background baryon density, the speed of sound and the background pressure in the medium respectively where perturbation propagates. Equations (13) and (21) can be rewritten using (23) as follows

$$\frac{\partial\rho}{\partial t} + c_s v_x \frac{\partial\rho}{\partial x} + c_s \rho \frac{\partial v_x}{\partial x} = 0 \tag{24}$$

$$\begin{aligned} \rho\left(\frac{\partial v_x}{\partial t} + c_s v_x \frac{\partial v_x}{\partial x}\right) \quad = \quad & \frac{\rho_0}{M c_s}\left(7.5 - \frac{g_\omega^2}{m_\omega^2} - 16\frac{m_\sigma^2}{g_\sigma^2} - 15.2\frac{\kappa}{g_\sigma^3} - 10.84\frac{\lambda}{g_\sigma^4}\right) \\ & \rho\frac{\partial\rho}{\partial x} - \frac{\rho_0^2}{M c_s}\left(127.56\frac{\kappa}{g_\sigma^3} + 182.1\frac{\lambda}{g_\sigma^4}\right) \\ & \rho^2\frac{\partial\rho}{\partial x} - \frac{\rho_0^3}{M c_s}\left(764.76\frac{\lambda}{g_\sigma^4}\right)\rho^3\frac{\partial\rho}{\partial x} \\ & +5.42\frac{\rho_0^{\frac{5}{3}}}{M c_s}\rho^{\frac{5}{3}}\frac{\partial\rho}{\partial x} + 2.9\frac{\rho_0^{\frac{2}{3}}}{M c_s}\rho^{\frac{2}{3}}\frac{\partial\rho}{\partial x} \\ & +0.33\frac{\rho_0^{-\frac{1}{3}}}{M c_s}\rho^{-\frac{1}{3}}\frac{\partial\rho}{\partial x} + \frac{1}{M\rho_0}\left(\zeta + \frac{4}{3}\nu\right)\frac{\partial^2 v_x}{\partial x^2} \end{aligned} \tag{25}$$

If the dimensionless baryon density and the fluid velocity are expanded around their equilibrium values, we have:

$$\rho = 1 + \sigma^2\rho_1 + \sigma^3\rho_2 + \sigma^4\rho_3 + \dots \tag{26}$$

$$v = \sigma^2 v_1 + \sigma^3 v_2 + \sigma^4 v_4 + \dots \tag{27}$$

Substituting equations (26) and (27) into equations (24) and (25), neglecting the terms proportional to $\sigma^{\geq 3}$ for first non-zero order of equations (24) and (25) will lead to

$$c_s\frac{\partial v_1}{\partial\xi} + c_s\frac{\partial v_1}{\partial\eta} - c_1\frac{\partial\rho_1}{\partial\xi} + c_2\frac{\partial\rho_1}{\partial\eta} = 0 \tag{28}$$

$$\begin{aligned} -c_1\frac{\partial v_1}{\partial\xi} + c_2\frac{\partial v_1}{\partial\eta} \quad - \quad & \left[\frac{\rho_0}{M c_s}\left(7.5 - \frac{g_\omega^2}{m_\omega^2} - 16\frac{m_\sigma^2}{g_\sigma^2} - 15.2\frac{\kappa}{g_\sigma^3} - 10.84\frac{\lambda}{g_\sigma^4}\right)\right. \\ & \left. -\frac{\rho_0^2}{M c_s}\left(127.56\frac{\kappa}{g_\sigma^3} + 182.1\frac{\lambda}{g_\sigma^4}\right) - \frac{\rho_0^3}{M c_s}\left(764.76\frac{\lambda}{g_\sigma^4}\right)\right. \end{aligned}$$

$$+5.42\frac{\rho_0^{\frac{5}{3}}}{Mc_s}-2.9\frac{\rho_0^{\frac{2}{3}}}{Mc_s}\rho^{\frac{2}{3}}-0.33\frac{\rho_0^{-\frac{1}{3}}}{Mc_s}\,]$$
$$\left(\frac{\partial\rho_1}{\partial\xi}+\frac{\partial\rho_1}{\partial\eta}\right)=0 \tag{29}$$

Dependencies of ρ_1 and v_1 to the ξ, η and τ can be considered as $\rho_1=\rho_1^1(\xi,\tau)+\rho_1^2(\eta,\tau)$ and $v_1=v_1^1(\xi,\tau)+v_1^2(\eta,\tau)$. If these expressions are inserted into equations (28) and (29) then we will have the following:

$$c_s\frac{\partial v_1^1}{\partial\xi}+c_s\frac{\partial v_1^2}{\partial\eta}-c_1\frac{\partial\rho_1^1}{\partial\xi}+c_2\frac{\partial\rho_1^2}{\partial\eta}=0 \tag{30}$$

$$\begin{aligned}-c_1\frac{\partial v_1^1}{\partial\xi}+c_2\frac{\partial v_1^2}{\partial\eta} \quad - \quad & \left[\frac{\rho_0}{Mc_s}\left(7.5-\frac{g_\omega^2}{m_\omega^2}-16\frac{m_\sigma^2}{g_\sigma^2}-15.2\frac{\kappa}{g_\sigma^3}-10.84\frac{\lambda}{g_\sigma^4}\right)\right.\\
& -\frac{\rho_0^2}{Mc_s}\left(127.56\frac{\kappa}{g_\sigma^3}+182.1\frac{\lambda}{g_\sigma^4}\right)-\frac{\rho_0^3}{Mc_s}\left(764.76\frac{\lambda}{g_\sigma^4}\right)\\
& +5.42\frac{\rho_0^{\frac{5}{3}}}{Mc_s}-2.9\frac{\rho_0^{\frac{2}{3}}}{Mc_s}\rho^{\frac{2}{3}}-0.33\frac{\rho_0^{-\frac{1}{3}}}{Mc_s}\,]\\
& \left(\frac{\partial\rho_1^1}{\partial\xi}+\frac{\partial\rho_1^1}{\partial\eta}\right)=0\end{aligned} \tag{31}$$

In this way the fluid velocity becomes

$$v_1=\frac{1}{c_s}\left(c_1\rho_1^1(\xi,\tau)-c_2\rho_1^2(\eta,\tau)\right) \tag{32}$$

and the phase velocities are obtained as

$$\begin{aligned}c_1^2=c_2^2 \quad = \quad & -\frac{\rho_0}{M}\left(7.5-\frac{g_\omega^2}{m_\omega^2}-16\frac{m_\sigma^2}{g_\sigma^2}-15.2\frac{\kappa}{g_\sigma^3}-10.84\frac{\lambda}{g_\sigma^4}\right)\\
& +\frac{\rho_0^2}{M}\left(127.56\frac{\kappa}{g_\sigma^3}+182.1\frac{\lambda}{g_\sigma^4}\right)+\frac{\rho_0^3}{M}\left(764.76\frac{\lambda}{g_\sigma^4}\right)\\
& -5.42\frac{\rho_0^{\frac{5}{3}}}{M}+2.9\frac{\rho_0^{\frac{2}{3}}}{M}\rho^{\frac{2}{3}}+0.33\frac{\rho_0^{-\frac{1}{3}}}{M}\end{aligned} \tag{33}$$

The second order equations respect to σ in (24) and (25) lead to the same results by replacing index "1" by " 2" and vice versa. Inserting equations (32) and (33) into equations (24) and (25) and collecting third order terms with respect to σ results in:

$$\begin{aligned}&\frac{\partial\rho_1^1}{\partial\tau}+\frac{\partial\rho_1^2}{\partial\tau}-c_1\frac{\partial\rho_3}{\partial\xi}+c_2\frac{\partial\rho_3}{\partial\eta}-2c_2Q_{0\xi}\frac{\partial\rho_1^2}{\partial\eta}+2c_1P_{0\eta}\frac{\partial\rho_1^1}{\partial\xi}+\\
&c_s\frac{\partial v_3}{\partial\xi}+c_s\frac{\partial v_3}{\partial\eta}+2c_1\rho_1^1\frac{\partial\rho_1^1}{\partial\xi}-2c_1\rho_1^2\frac{\partial\rho_1^2}{\partial\eta}=0\end{aligned} \tag{34}$$

and

$$-c_1\frac{\partial v_3}{\partial\xi}+c_2\frac{\partial v_3}{\partial\eta}+\frac{2c_1^2}{c_s}P_{0\eta}\frac{\partial\rho_1^1}{\partial\xi}+\frac{2c_2^2}{c_s}Q_{0\xi}\frac{\partial\rho_1^2}{\partial\eta}+\frac{c_1}{c_s}\frac{\partial\rho_1^1}{\partial\tau}-\frac{c_2}{c_s}\frac{\partial\rho_1^2}{\partial\tau}$$

$$
\begin{aligned}
&-\frac{1}{M\rho_0}\left(\widetilde{\zeta}+\frac{4}{3}\widetilde{\upsilon}\right)\left[\frac{c_1}{c_s}\frac{\partial^2\rho_1^1}{\partial\xi^2}-\frac{c_2}{c_s}\frac{\partial^2\rho_1^2}{\partial\eta^2}\right]+\frac{c_1^2}{c_s}\frac{\partial\rho_3}{\partial\xi}+\frac{c_2^2}{c_s}\frac{\partial\rho_3}{\partial\eta}\\
&+\left[\frac{\rho_0^2}{Mc_s}\left(127.56\frac{\kappa}{g_\sigma^3}+182.1\frac{\lambda}{g_\sigma^4}\right)+\frac{\rho_0^3}{Mc_s}\left(1529.52\frac{\lambda}{g_\sigma^4}\right)\right.\\
&\left.-3.61\frac{\rho_0^{\frac{5}{3}}}{Mc_s}+0.97\frac{\rho_0^{\frac{2}{3}}}{Mc_s}-0.44\frac{\rho_0^{-\frac{1}{3}}}{Mc_s}+\frac{c_1^2}{c_s}\right]\left(\rho_1^1\frac{\partial\rho_1^1}{\partial\xi}+\rho_1^2\frac{\partial\rho_1^1}{\partial\eta}\right)\\
&+\left[\frac{\rho_0^2}{Mc_s}\left(127.56\frac{\kappa}{g_\sigma^3}+182.1\frac{\lambda}{g_\sigma^4}\right)+\frac{\rho_0^3}{Mc_s}\left(1529.52\frac{\lambda}{g_\sigma^4}\right)\right.\\
&\left.-3.61\frac{\rho_0^{\frac{5}{3}}}{Mc_s}+0.97\frac{\rho_0^{\frac{2}{3}}}{Mc_s}-0.44\frac{\rho_0^{-\frac{1}{3}}}{Mc_s}-\frac{c_1^2}{c_s}\right]\\
&\left(\rho_1^1\frac{\partial\rho_1^2}{\partial\eta}+\rho_1^2\frac{\partial\rho_1^1}{\partial\xi}\right)=0
\end{aligned}
\tag{35}
$$

where $\widetilde{\zeta}$ and $\widetilde{\upsilon}$ are small perturbation in viscosities. Differentiating equations (34) and (35) with respect to ξ and η and performing some calculations the following equations obtain:

$$
\frac{\partial\rho_1^1}{\partial\tau}+\frac{c_1}{2}\left(3+\Re\right)\rho_1^1\frac{\partial\rho_1^1}{\partial\xi}-\frac{1}{2M\rho_0}\left(\widetilde{\zeta}+\frac{4}{3}\widetilde{\upsilon}\right)\frac{\partial^2\rho_1^1}{\partial\xi^2}=0 \tag{36}
$$

$$
\begin{aligned}
\frac{\partial\rho_1^2}{\partial\tau}-\frac{c_1}{2}\left(3+\Re\right)\rho_1^2\frac{\partial\rho_1^2}{\partial\eta} \quad &- \quad \frac{1}{2M\rho_0}\left(\widetilde{\zeta}+\frac{4}{3}\widetilde{\upsilon}\right)\frac{\partial^2\rho_1^2}{\partial\eta^2}\\
&-2c_1\left(\Re-1\right)\rho_1^2\frac{\partial\rho_1^1}{\partial\xi}=0
\end{aligned}
\tag{37}
$$

$$
P_{0\eta}=\frac{1}{4}\left(1-\Re\right)\rho_1^2 \tag{38}
$$

$$
Q_{0\xi}=\frac{1}{4}\left(1-\Re\right)\rho_1^1 \tag{39}
$$

where $\Re$ is introduced as following expression

$$
\begin{aligned}
\Re \quad = \quad &\frac{1}{c_1^2}\left[\frac{\rho_0^2}{Mc_s}\left(127.56\frac{\kappa}{g_\sigma^3}+182.1\frac{\lambda}{g_\sigma^4}\right)+\frac{\rho_0^3}{Mc_s}\left(1529.52\frac{\lambda}{g_\sigma^4}\right)\right.\\
&\left.-3.61\frac{\rho_0^{\frac{5}{3}}}{Mc_s}+0.97\frac{\rho_0^{\frac{2}{3}}}{Mc_s}-0.44\frac{\rho_0^{-\frac{1}{3}}}{Mc_s}\right]
\end{aligned}
\tag{40}
$$

Equations (36) and (37) are the Burgers equations in (ξ,τ) and (η,τ) space, $P_{0\eta}$ and $Q_{0\xi}$ are the phase shifts of the localized waves after their head on collision respectively. For two shock waves that moved toward each other in the (x,t) space we have

$$
\begin{aligned}
&\frac{\partial\widehat{\rho}_1^1}{\partial t}+c_1\frac{\partial\widehat{\rho}_1^1}{\partial x}+\frac{c_1}{2}\left(3+\Re\right)\widehat{\rho}_1^1\frac{\partial\widehat{\rho}_1^1}{\partial x}-\frac{1}{2M\rho_0}\left(\zeta+\frac{4}{3}\upsilon\right)\frac{\partial^2\widehat{\rho}_1^1}{\partial x^2}+\\
&+\frac{1}{4}\left(1-\Re\right)\widehat{\rho}_1^2\left[\frac{\partial\widehat{\rho}_1^1}{\partial t}-c_1\frac{\partial\widehat{\rho}_1^1}{\partial x}+\frac{1}{2M\rho_0}\left(\zeta+\frac{4}{3}\upsilon\right)\frac{\partial^2\widehat{\rho}_1^1}{\partial x^2}\right]=0
\end{aligned}
\tag{41}
$$

This is the Burgers equation for $\widehat{\rho}_1^1\equiv\sigma^2\rho_1^1$, which is a small localized perturbation in the baryon density moving towards the right. The following equation describes a moving

perturbation propagates in inviscid medium with $\zeta = \upsilon = 0$

$$\frac{\partial \widehat{\rho}_1^1}{\partial t} + c_1 \frac{\partial \widehat{\rho}_1^1}{\partial x} + \frac{c_1}{2}(3+\Re)\,\widehat{\rho}_1^1 \frac{\partial \widehat{\rho}_1^1}{\partial x} + \frac{1}{4}(1-\Re)\,\widehat{\rho}_1^2 \left[\frac{\partial \widehat{\rho}_1^1}{\partial t} - c_1 \frac{\partial \widehat{\rho}_1^1}{\partial x}\right] = 0 \tag{42}$$

This equation is called the breaking wave equation. Similarly, the Burgers equation for $\widehat{\rho}_1^2 \equiv \sigma^2 \rho_1^2$ becomes

$$\begin{aligned}
&\frac{\partial \widehat{\rho}_1^2}{\partial t} - c_1 \frac{\partial \widehat{\rho}_1^2}{\partial x} - \frac{c_1}{2}(3+\Re)\,\widehat{\rho}_1^2 \frac{\partial \widehat{\rho}_1^2}{\partial x} - \frac{1}{2M\rho_0}\left(\zeta + \frac{4}{3}\upsilon\right)\frac{\partial^2 \widehat{\rho}_1^2}{\partial x^2} \\
&+\frac{1}{4}(1-\Re)\,\widehat{\rho}_1^1 \left[\frac{\partial \widehat{\rho}_1^2}{\partial t} + c_1 \frac{\partial \widehat{\rho}_1^2}{\partial x} + \frac{1}{2M\rho_0}\left(\zeta + \frac{4}{3}\upsilon\right)\frac{\partial^2 \widehat{\rho}_1^2}{\partial x^2}\right] \\
&+\left[c_1(1-\Re) + \frac{c_1}{2}(1-\Re)^2\left[\widehat{\rho}_1^1 - \widehat{\rho}_1^2\right]\right]\widehat{\rho}_1^2 \frac{\partial \widehat{\rho}_1^1}{\partial x} = 0
\end{aligned} \tag{43}$$

which is a small perturbation in the baryon density that moves to the left. The breaking wave equation for $\widehat{\rho}_1^2$ moving in inviscid media can be found by inserting $\zeta = \upsilon = 0$ in the equation (43) as

$$\begin{aligned}
&\frac{\partial \widehat{\rho}_1^2}{\partial t} - c_1 \frac{\partial \widehat{\rho}_1^2}{\partial x} - \frac{c_1}{2}(3+\Re)\,\widehat{\rho}_1^2 \frac{\partial \widehat{\rho}_1^2}{\partial x} \\
&+\frac{1}{4}(1-\Re)\,\widehat{\rho}_1^1 \left[\frac{\partial \widehat{\rho}_1^2}{\partial t} + c_1 \frac{\partial \widehat{\rho}_1^2}{\partial x}\right] \\
&+\left[c_1(1-\Re) + \frac{c_1}{2}(1-\Re)^2\left[\widehat{\rho}_1^1 - \widehat{\rho}_1^2\right]\right]\widehat{\rho}_1^2 \frac{\partial \widehat{\rho}_1^1}{\partial x} = 0
\end{aligned} \tag{44}$$

Now we have found the main equations which describe head-on collision of localized waves in dense hadronic media. The above equations don't have known analytical solutions and therefore we have to solve them numerically.

IV. Numerical Discussion

We can rewrite the Burgers equations (41) and (43) in the general form

$$\frac{\partial \widehat{\rho}}{\partial t} + c\frac{\partial \widehat{\rho}}{\partial x} + \alpha \widehat{\rho}\frac{\partial \widehat{\rho}}{\partial x} = \mu \frac{\partial^2 \widehat{\rho}}{\partial x^2} \tag{45}$$

where $\alpha = \pm\frac{c_1}{2}(3+\Re)$ and μ are the respective nonlinear and dissipative coefficients for hadron phase. The dissipative coefficient μ is related to the viscosity. Since the Burgers equations dont have any exact solution, we use localized solutions of the Korteweg-de Vries (KdV) equation as an initial condition for numerical calculations. Hence, localized soliton-like structure $\rho(x, t=0) = A sech(\frac{x}{L})$ are proposed as initial condition, where the initial amplitude is A and L denotes its width. Time evolution of this soliton-like solution simulates the evolution of a localized perturbation in viscous hadronic gas. Phase velocities are important parameters in head on collision which are described by equation (33). This equation shows that they have intricate relation with the medium parameters. Figure 1 presents the phase velocity c_1 of colliding waves as a function ρ_0 . As might be expected, phase velocities increase as the medium density increases. This figure also shows that in a small range of background density, phase velocity is almost a linear function of ρ_0 . Phase shifts are the other important parameters in head on collision. Calculated values of these parameters in

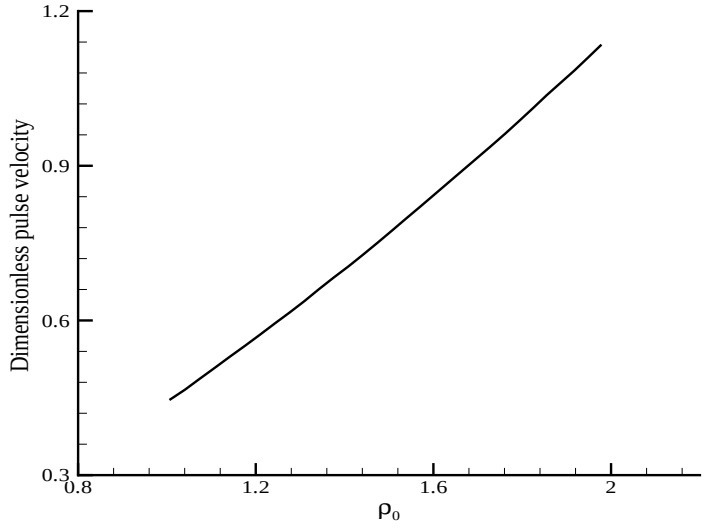

Figure 1: The phase velocity of propagated waves as a function of back ground density. Values of the other parameters have been given in the text

our problem have been presented by equations (38) and (39). These equations clearly show that they are negative because in hadron gas $\Re > 1$. Figure 2 demonstrates time evolution of the colliding waves during their interaction in a inviscid medium. Simulations clearly show that the phase velocities of the localized waves are almost the same. Figure 2 shows that the localized waves are changed into shock profiles while traveling in the medium. This figure also presents that the needed time to change a soliton into a shock profile becomes smaller when the initial waves have larger amplitude. Effects of viscosity on the evolution of waves during their collision have been presented in the figure 3. This figure clearly illustrates that the viscosity is able to control the creation of shock waves in the medium. Definitely the term with second order of derivation in the equations (41) and (43) reduces the non-linearity effects in a way that the shock profiles are created very late. In addition, viscosity causes a noticeable damping on the wave amplitude which is an important result. The traveling distance of localized perturbations in a medium helps us to find valuable information about the amount of viscosity of the medium. Comparing the traveling distance of such waves in media with different initial conditions give us a qualitative information about the shock profile. The figure 3 also shows that the amplitude and width of localized waves approximately remain constant in the viscid media.

V. Conclusions and Remarks

Propagation of solitary waves in cold and dense hadronic matter is studied in this work. It is expected to find such media in the core of neutron and compact stars. Hydrodynamic description and equation of state of such viscose fluid leaded us to find a nonlinear differential equation for propagation of localized perturbation which is called the Burgers equation. Viscosity is able to control the nonlinear effects so that it can postpone the shock profiles. It is shown that the amplitude and width of propagated solitary waves in viscose hadronic

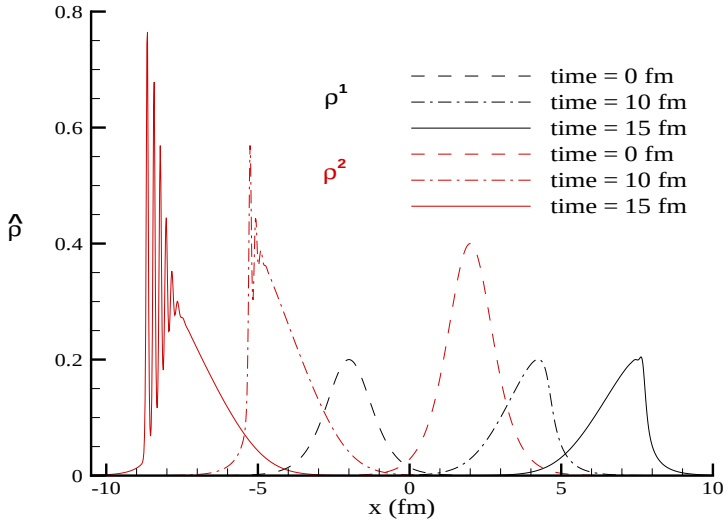

Figure 2: Wave profiles before and head on collision in non-viscous medium.

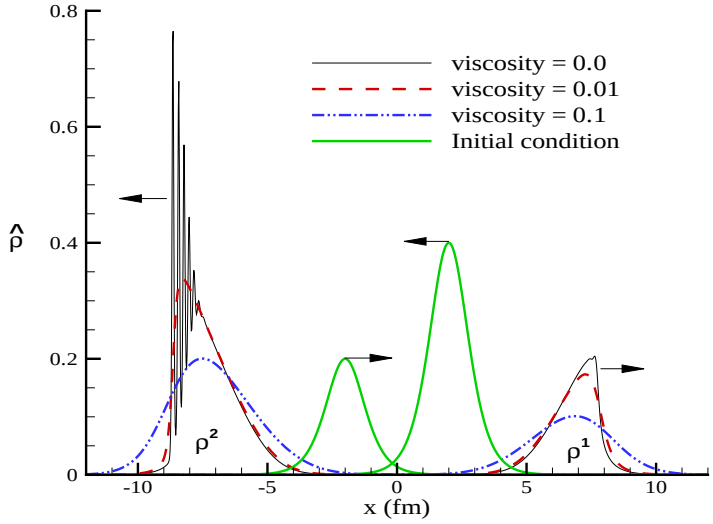

Figure 3: Wave profiles before and head on collision in viscous media with different viscosities.

medium remain approximately constant during and after the collision. The phase shifts of propagating waves after the collision are always negative. These phase shifts are functions of initial background density and characterize by the medium particles, but independent of the viscosity. It is interesting to investigate such media with finite temperature. For this purpose it is better to construct a more suitable EoS for this medium which can be studied in the future works. Since the EoS of the QGP phase in finite temperature is different, the same investigations for this medium should be considered.

References

[1] I. Mishustina, et al., Phase transition in compact stars due to a violent shock, Phys. Rev. C **91** (2015) 055806.

[2] P. K. Panda, H. S. Nataraj, Rotating compact star with superconducting quark matter, Phys. Rev. C **73** (2006) 025807.

[3] S. Weissenborn, et al., Hyperons and massive neutron stars: the role of hyperon potentials, Nucl. Phys. A **881** (2012) 62-77.

[4] J. Schaffner-Bielich, et al., Astrophysical implications of the QCD phase transition, PoS. Confinement. **8** (2009) 138.

[5] S. Schramm, et al., Structure and cooling of neutron and hybrid stars, arXiv:1202.5113 [astro-ph.SR].

[6] W. H. Y. Wang, et al., The third family of compact stars with the color-flavor locked quark core, Chin. Sci. Bull. **58** (2013) 3731-3734.

[7] R. E.Pudritz, et al., Shock interactions, turbulence and the origin of the stellar mass spectrum, Phil. Trans. R. Soc. A **371** (2013) 2003.

[8] J. Macher, J. Schaffner-Bielich, Phase transitions in Compact Stars, Eur. J. Phys. **26** (2005) 341-360.

[9] D. Logoteta, et al., Formation of hybrid stars from metastable hadronic stars,Phys. Rev. C**88** (2013) 5,055802.

[10] D. Logoteta, et al., Quark matter nucleation with a microscopic hadronic equation of state, Phys. Rev. C **85** (2012) 055807.

[11] H. R. Moshfegh, et al., Cold Hybrid star properties, AIP Conf. Proc.**1377** (2011) 405.

[12] G. Peilert, et al., Physics of high-energy heavy-ion collisions, Rep. Prog. Phys.**57** (1994) 533-602.

[13] S. Floerchinger, et al., A perturbative approach to the hydrodynamics of heavy ion collisions, Nucl. Phys. A**931** (2014) 965-9.

[14] I. Kozlov, et al., Signatures of collective behavior in small systems, Nucl. Phys. A**931** (2014) 1045-50.

[15] D.A. Fogaca, F.S. Navarra, L.G. Ferreira Filho, Viscosity, wave damping and shock wave formation in cold hadronic matter, Phys. Rev C **88** (2013) 025208.

[16] P. Huovinen, P.V. Ruuskanen, Hydrodynamic models for heavy ion collisions, Annu. Rev. Nucl. Part. Sci. **56** (2006) 163-206.

[17] A. Bazavov, The QCD equation of state, Nucl. Phys. A**931** (2014) 851-5.

[18] H. Niemi, Collective dynamics in relativistic nuclear collisions, Nucl. Phys. A **931** (2014) 227-37.

[19] D.A. Fogaca, F.S. Navarra, L.G. Ferreira Filho, Nonlinear waves in a Quark Gluon Plasma, Phys. Rev. C**81** (2010) 055211.

[20] D.A. Fogaca, F.S. Navarra, L.G. Ferreira Filho, Kadomtsev-Petviashvili equation in relativistic fluid dynamics, Commun. Nonlinear. Sci. **18** (2013) 221-35.

[21] J. I. Kapusta, et al., Relativistic theory of hydrodynamic fluctuations with applications to heavy-ion collisions, Phys. Rev. C **85** (2012) 054906.

[22] P. Staig, E. Shuryak, The fate of the initial state fluctuations in heavy ion collisions , Phys. Rev. C **84** (2011) 034908.

[23] Z. Qiu, U. Heinz, Event-by-event shape and flow fluctuations of relativistic heavy-ion collision fireballs, Phys. Rev. C **84** (2011) 024911.

[24] H. Demiray, Head-on collision of solitary waves in fluid-filled elastic tubes, Appl. Math. Lett.**18** (2005) 941-50.

[25]T. Tsuboi, Phase shift in the collision of two solitons propagating in a nonlinear transmission line, Phys. Rev.A **40** (1989) 2753-5.

[26] E.F. El-Shamy, et al., Head-on collision of ion-acoustic solitary waves in multicomponent plasmas with positrons, Phys. Plasmas. **17** (2010) 082311.

[27] E.F. El-Shamy, W.A. Awad, on the characteristics of the head-on collision between two ion thermal waves in isothermal pair-ion plasmas containing charged dust grains, Chaos. Soliton. Fract. **45** (2012) 1520.

[28] W. Wen, G. Huang, Dynamics of dark solitons in superfluid Fermi gases in the BCS-BEC crossover, Phys. Rev.A **79** (2009) 023605.

[29] M.G. Paoli. D.P. Menezes, The importance of the mixed phase in hybrid stars built with the Nambu-Jona-Lasinio model, Eur. Phys. J. A **46** (2010) 413-20.

[30] D. Logoteta, et al., A chiral model approach to quark matter nucleation in neutron stars, Phys. Rev. D **85** (2012) 023003.

[31] I. Bombaci, et al., Metastability of hadronic compact stars, Phys. Rev. D **77** (2008) 083002.

[32] B.D. Serot, Building atomic nuclei with the Dirac equation, Int. J. Mod. Phys. A **19S1** (2004) 107-120.

[33] F. Verheest, et al., Head-on collisions of electrostatic solitons in nonthermal plasmas, Phys. Rev. E **86** (2012) 036402.